0013-7227/06/$15.00/0
Printed in U.S.A.

Endocrinology 147(1):155–165
Copyright © 2006 by The Endocrine Society
doi: 10.1210/en.2005-0386

Expression of the Insulin Receptor-Related Receptor Is Induced by the Preovulatory Surge of Luteinizing Hormone in Thecal-Interstitial Cells of the Rat Ovary

Gregory A. Dissen, Cecilia Garcia-Rudaz, Veronica Tapia, Luis F. Parada, Sheau-Yu Teddy Hsu, and Sergio R. Ojeda

Division of Neuroscience (G.A.D., C.G.-R., V.T., S.R.O.), Oregon National Primate Research Center/Oregon Health & Science University, Beaverton, Oregon 97006-3448; Center for Developmental Biology (L.F.P.), University of Texas Southwestern Medical Center, at Dallas, Dallas, Texas 75390-9133; and Division of Reproductive Biology (S.-Y.T.H.), Department of OB/GYN, Stanford University School of Medicine, Stanford, California 94305

The insulin receptor-related receptor (IRR) is a member of the insulin receptor family that, on its own, recognizes neither insulin nor any of the identified insulin-related peptides. In both the nervous system and peripheral tissues, IRR mRNA is detected in cells that also express trkA, the nerve growth factor tyrosine kinase receptor. In the ovary, the *trkA* gene is transiently activated in thecal-interstitial cells of large antral follicles at the time of the preovulatory surge of gonadotropins. The present study shows that the *IRR* gene is expressed in the same ovarian compartment, that IRR mRNA content increases strikingly in these cells in the afternoon of the first proestrus, and that—as in the case of trkA mRNA—the increase is caused by gonadotropins. The IRR mRNA species primarily affected is that encoding the full-length receptor; its increased abundance was accompanied by a corresponding change in IRR protein content. An extensive molecular search using several approaches, including the screening of cDNA libraries and PCR amplification with degenerate primers, did not yield an IRR ligand. Phylogenetic analysis of 20 insulin-related sequences and 15 relaxin family peptides from selected vertebrates indicated that the mammalian genome is unlikely to contain an additional ligand expressed from a distinct gene that is closely related to the insulin family. Although the functional nature of the relationship between IRR and trkA receptors is unknown, the remarkable temporal and spatial specificities of their coordinated expression in the ovary before ovulation suggests that they target a functionally related set of downstream events associated with the ovulatory process. (*Endocrinology* 147: 155–165, 2006)

THE INSULIN RECEPTOR-related receptor (IRR) is an orphan receptor of the insulin receptor (IR) tyrosine kinase family, identified due to its similarity to the IR (1). The human and guinea pig IRR consists of two subunits (α and β) derived from a single proreceptor molecule that is cleaved during processing (1, 2). The structure of mouse (3) and rat (4, 5) IRR is essentially the same. The α subunit consists of a 716 amino acid polypeptide of molecular weight (M_r) 108,000, and the β subunit consists of a 551 amino acid polypeptide of M_r 66,000 (1, 6). The two subunits are connected by intermolecular disulfide bonds. Whereas the α subunit determines ligand specificity and contains a cysteine-rich domain located toward the amino terminus that is required for ligand binding (7, 8), the β subunit comprises the remainder of the receptor, including an extracellular, transmembrane, and intracellular domain. The latter contains the tyrosine kinase-encoding region of the receptor. In addition to the full-length receptor, there are two truncated forms that result from alternative splicing of the primary mRNA transcript (9). These truncated forms (sIRR-1 and sIRR-2) are polypeptides containing 410 and 469 amino acids, respectively (M_r 49,000 and 53,000); they contain the cysteine-rich ligand-binding domain of the receptor but cannot associate with the β subunit and, thus, are thought to be secreted (9).

Noteworthy, the *IRR* gene is located approximately 2 kb and in the opposite transcriptional orientation from that of the *trkA* gene, which encodes the high-affinity nerve growth factor (NGF) receptor (10–12). This relationship is conserved in humans, rats, and mice, wherein the genes are located on chromosomes 1 (13, 14) (GenBank accession numbers: IRR, NM_014215; trkA, NM_002529), 2 (IRR, NM_022212; trkA, NM021589), and 3 (IRR, NM_011832; trkA, XM_283871), respectively. In addition to the *IRR* and *trkA* genes being near to each other in the genome, the receptors have been shown to be coexpressed in both the peripheral and central nervous system (15, 16). Cholinergic neurons of the basal forebrain (17, 18) provide a remarkable example of this coexpression. In addition to the nervous system, the IRR and trkA receptors are found in kidney (5, 19–24), pancreas (3, 22, 25, 26), and thymus (4, 22, 27, 28). These findings suggest that the expression of both of the receptors might be coregulated by similar factors; however, none of such factors has been identified.

We previously showed that trkA mRNA abundance in the ovary increases markedly in thecal-interstitial cells at the

First Published Online September 29, 2005

Abbreviations: IGF-Rs, IGF receptors; IGF-IR, IGF-I receptor; IR, insulin receptor; IRR, IR-related receptor; IRS, IR substrate; M_r, molecular weight; NGF, nerve growth factor; nt, nucleotide(s); PMSG, pregnant mare serum gonadotropin; RPA, RNase protection assay.

***Endocrinology* is published monthly by The Endocrine Society (http://www.endo-society.org), the foremost professional society serving the endocrine community.**

Downloaded from https://academic.oup.com/endo/article/147/1/155/2500201 by Universidad de Chile user on 05 August 2022

time of the preovulatory surge of LH (29). This increase is transient, occurs in a temporally and spatially restricted manner, and is brought about by the preovulatory LH surge, indicating that expression of the *trkA* gene in reproductively competent ovaries is a tightly regulated event. We now report that expression of the *IRR* gene in the preovulatory ovary also increases abruptly in the afternoon of proestrus in thecal-interstitial cells and that, as in the case of trkA, the increase is gonadotropin dependent. We also present results of an extensive molecular and bioinformatics search suggesting that an IRR ligand may not exist as a separate, IR ligand-related gene in the mammalian genome. These findings lend additional support to the view that IRR may function as a auxiliary member of the IR family (30) and raise the possibility that such role may extend to coexpressed recognition molecules, such as the trkA receptor.

Materials and Methods

Animals

Sprague Dawley rats (B&K Universal, Fremont, CA) were housed under controlled conditions of temperature (23–25 C) and light (14-h light, 10-h dark; lights on from 0500–1900 h). Food (Purina laboratory chow, Ralston-Purina, St. Louis, MO) and water were provided *ad libitum*. Animal usage was duly approved by the Institutional Animal Care and Use Committee of the Oregon National Primate Research Center.

In vivo procedures

To characterize the pattern of *IRR* gene expression at the time of puberty, the ovaries were collected at the end of the juvenile period (postnatal d 28–29) and during the peripubertal phase (d 32–40). Peripubertal rats were classified in different phases of puberty (juvenile, early proestrus, late proestrus, estrus, and diestrus) according to criteria previously reported (31). All ovaries were collected at 1700 h, because we have previously shown that in Sprague Dawley rats the LH surge is initiated by 1400 h of the day of first proestrus, becoming maximal between 1600–1800 h (32). To accelerate ovarian development and induce a preovulatory LH surge, juvenile rats were given a single sc injection of pregnant mare serum gonadotropin (PMSG) (8 IU/rat) on d 26–27 of age, and the ovaries were collected at 2-h intervals between 1500–2300 h on the expected day of the preovulatory LH surge. The first set of ovaries was collected 54 h after the administration of PMSG (*i.e.* at 1500 h). In one experiment, granulosa cells were separated from the rest of the ovary [termed residual ovary; (33)] by puncturing the follicles with a 23-gauge needle and expressing the granulosa cells into DMEM (Sigma, St. Louis, Mo).

RT-PCR cloning

Total RNA for both RT-PCR cloning (IRR and cyclophilin cDNAs) and RNase protection assay (RPA) (see below) was prepared by the acid phenol-extraction method (34).

The cDNA templates used to prepare cRNA probes for RPA were produced by RT of total RNA (IRR, 1 μg of kidney RNA; cyclophilin, 200 ng of ovary RNA) using Superscript II reverse transcriptase (Life Technologies, Grand Island, NY) and an oligo-deoxythymidine primer (5′-GACTCGAGGATCCATCGA-T_{18}-3′) containing sequences for *Xho*I, *Bam*HI, and *Cla*I restriction sites at its 5′ end. The RT reaction was carried out at 42 C for 1 h followed by 30 min at 52 C. The subsequent PCR used 5% of the RT reaction and a set of 20-mer oligodeoxynucleotides intended to amplify a 428-bp segment of IRR mRNA (4) (GenBank accession no. M90661). The sense primer (5′-CTGGGTGAGGAGTGTGCTGA-3′) corresponds to nucleotides (nt) 912–931 in the IRR mRNA sequence; the antisense primer (5′-CTGCTGCCATTACGGGTGAA-3′) is complementary to nt 1320–1339. The primers used to amplify cyclophilin were a sense primer (5′-GGGAAGTCCATCTACGGA-3′) corresponding to nt 265–282 and an antisense primer (5′-ACATGCTTGCCATCCAAC-3′) complementary to nt 405–422 in rat cyclophilin (35) (GenBank accession no. M19533). The PCR conditions used have been described previously (36). The resulting 428-bp IRR PCR product corresponds to a segment in IRR mRNA encoding a portion of the cysteine-rich, putative binding domain in the α subunit of IRR (1). This cDNA includes sequences from both exon 2 and exon 3. The cyclophilin PCR product was 158 bp. The PCR products were cloned into the pGEM-T vector (Promega, Madison, WI). Their identity was confirmed by either restriction endonuclease digestion using at least three diagnostic restriction endonucleases or by sequencing.

Because IRR has two splice variants that encode truncated and secreted forms of the receptor (9), an additional IRR cDNA was generated to differentiate, via RPA, the full-length mRNA from the splice variants sIRR-1 and sIRR-2. The PCR amplification was carried out as described above with a set of 24-mer oligodeoxynucleotides intended to amplify a 554-bp segment of IRR mRNA (4). The sense primer (5′-CCGGGCACCTACCAGTATGAGTCT-3′) corresponds to nt 1188–1211 in the IRR mRNA sequence; the antisense primer (5′-AGGCGTGGGTTGAAGGCGAAGTAT-3′) is complementary to nt 1718–1741. The 5′ primer was located in exon 3, whereas the 3′ primer was located in exon 6 (4) spanning the splice variant region (9).

RNase protection assay

RPAs were carried out according to the method of Gilman (37), as previously described (38). Preparation of templates for transcription and the transcription procedure itself were performed as reported (39, 40). Cyclophilin mRNA, which is constitutively expressed in the ovary (41), was used as an internal control to normalize the gene-specific hybridization signals obtained. Sense RNA used for preparation of IRR mRNA standard curves was generated using the cDNA template described above. The sense RNA was transcribed, purified, and quantified according to published procedures (38). The ^{32}P-labeled IRR and cyclophilin cRNAs were simultaneously hybridized to total RNA extracted from tissues. After RNase digestion, the protected species were isolated by PAGE, visualized, and analyzed as reported (38). As described above, the RPA probe used for Figs. 1–3 and 5 extends from exon 2 to exon 3 and protects a fragment of 428 nt. The RPA probe used for the experiment described in Fig.4 extends from exon 3 to exon 6; it protects a 554-nt fragment corresponding to the full-length IRR mRNA. It can also protect fragments of 441 and 294 nt corresponding to the splice variants 1 and 2, respectively.

Quantitation of the IRR mRNA signals was performed as reported (42), *i.e.* first exposing the gel to Kodak Blue XB-1 film (Eastman Kodak Co, Rochester, NY) at −85 C and then analyzing the autoradiographic signals using a flatbed scanner and the computer program NIH-Image written by Dr. Wayne Rasband (National Institutes of Health, Bethesda, MD). An edited version of this program was provided by Dr. Cary Mariash (University of Minnesota, Minneapolis, MN); this version yields integrated optical densities following a user-specified method of subtraction of the background (29, 43). Thereafter, the sample signals were referred to those of a standard curve constructed with different concentrations of sense IRR mRNA hybridized to the IRR cRNA probe. Statistical analysis of the quantitative data consisted of ANOVA followed by Fisher's least-significant-difference procedure for comparison of individual means.

Western blots

Ovaries were collected from saline-treated juvenile rats (negative control), and age-matched rats treated with PMSG (collected at 2100 h, 2 d after PMSG injection). Kidney and liver tissue samples were collected and served as positive and negative controls, respectively. To measure IRR mRNA and protein levels in the ovaries from individual rats, total RNA from the left ovary of each rat was used for detection of IRR mRNA by RPA, whereas the right ovary and control tissues were employed for immunoblots. The tissues were homogenized and prepared for blotting as previously described (44). An 8% SDS-PAGE gel (4.5% stack) was loaded with 41 μg of ovarian protein and 50 μg of kidney and liver proteins. After transfer of the size-fractionated species to polyvinylidene difluoride membranes (Pierce, Rockford, IL) for 3 h at 4 C, the membranes were blotted with two different IRR antibodies (727 and 774), the characteristics of which have been previously reported (23).

Downloaded from https://academic.oup.com/endo/article/147/1/155/2500201 by Universidad de Chile user on 05 August 2022

Hybridization histochemistry

The procedure employed was based on the method of Simmons *et al.* (45) with modifications as reported (46). Cellular expression of IRR mRNA was determined in 14-μm cryostat sections of ovaries collected at 2100 h of the second day after a single PMSG injection and immediately fixed by immersion in 4% paraformaldehyde-0.1 M sodium borate buffer, pH 9.5 (overnight at 4 C). Thereafter, the ovaries were placed in 10% sucrose-PBS for 24 h at 4 C, embedded in optimal cutting temperature compound (Miles, Elkhart, IN) and frozen on dry ice before sectioning. After hybridization, the sections were exposed to NTB-2 emulsion (Roche, Indianapolis, IN), the radioactive signal was developed three weeks later, and the sections were counterstained with hematoxylin (Sigma). Control sections were incubated with a ^{32}P-labeled sense IRR RNA probe transcribed from the same cDNA template used to prepare antisense IRR RNA probe but transcribed from the opposite orientation.

Immunohistochemistry

Immunohistochemical detection of IRR was performed in 14-μm cryostat sections from ovaries collected at 2100 h, 2 d after PMSG. The ovaries were fixed by immersion in Zamboni's fixative, as described (42), and processed for IRR immunohistochemistry using the affinity-purified polyclonal antisera 727 and 774 (23). The antibodies were raised against synthetic peptides identical in sequence to portions of the juxtamembrane region (antibody 727) and the carboxy terminus [antibody 774 (23)]. Tissue sections were incubated overnight at 4 C with the antibodies at 2 μg/ml, and the immunoreaction was developed the next day using the diaminobenzidine procedure previously described (46).

Motif-based PCR with degenerate primers

The similarity of the IRR to IR and IGF receptors (IGF-Rs) suggested that a ligand for IRR would be of a similar nature or even a member of the insulin and relaxin family of ligands. Thus, peptide sequences of members of the insulin family were aligned to select areas of conserved motifs from which degenerate primers were then generated. RT reactions were carried out, as described above, using total RNA from kidney, stomach, brain, and ovary from both juvenile and late proestrus rats. The conditions for the PCRs were as described above, with the exception that the annealing temperature was varied from 50 to 60 C. In addition to using reverse-transcribed RNA as the starting template, cDNA libraries were used as the cDNA template for PCR amplification using the motif-based degenerated primers paired with λ-vector specific primers designed to the left or right arms of the λ phage DNA sequence. The cDNA libraries were prepared from RNA extracted from ovary, uterus, esophagus, colon, whole brain, hippocampus, basal forebrain, and liver. The libraries were produced by either our lab or were provided by Dr. Eliot Spindel (Oregon National Primate Research Center, Beaverton, OR), Dr. Srinivasa Nagalla (Oregon Health & Science University, Portland, OR), or Dr. Jim Boulter (University of California, Los Angeles, CA).

Screening of cDNA libraries

Two λ phage cDNA libraries (made from ovaries of rats in the first proestrus phase of the estrous cycle and from the adult rat hippocampus, mentioned above) were screened for the presence of the mammalian homolog of a novel cDNA sequence isolated from *Phyllomedusa sauvagei* (47) (the cDNA was the generous gift of Dr. Srinivasa Nagalla, Oregon Health & Science University). This cDNA encodes an insulin-like peptide with 54% similarity with human and 75% similarity with *Xenopus laevis* insulin prohormone at the amino acid level (47). The encoded peptide was considered to be an IRR ligand because of its biological activity. Synthetic peptides representing the A and B chains of the peptide and the peptide itself (expressed *in vitro* using rabbit reticulocyte lysates programmed with synthetic *P. sauvagei* mRNA) were able to stimulate autophosphorylation of the IR, IGF-IR, and IRR in cell lines stably transfected with each of these receptors (47). Both the ovarian and hippocampal libraries were screened (0.5–1 million clones from each library) (48, 49) using the ^{32}P-labeled cDNA random oligonucleotide-primed synthesis method (50).

Genomic search of insulin/relaxin peptide family genes and phylogenetic analysis of the IRR

Search of insulin and relaxin peptide family genes was initially started using the human insulin and relaxin precursors as the query for TBLASTN analyses of genomes from different model organisms. To identify all potential paralogous genes in different species, the statistical significance threshold for reporting matches against database sequences was set at a less stringent level using a higher EXPECT threshold. The putative insulin and relaxin family peptides from 20 insulin-related sequences and 15 relaxin family peptides from selected vertebrates were further verified based on the conserved arrangement of the six disulfide bridge-forming cysteines in the putative B and A mature domains. If available, the putative open reading frame was verified using expressed sequence tag or mRNA sequences in the GenBank. The Block Maker program (http://blocks.fhcrc.org) was used to align the mature peptides. Phylogenetic analysis was carried out using a routine in ClustalW (http://blocks.fhcrc.org/blocks/make_blocks.html).

To study the phylogenetic relationship among IR family proteins, sequences encoding the full-length proteins and the ectodomains of homologues from human, mouse, and frog *X. laevis* were downloaded from the GenBank and analyzed using the Block Maker program. In these analyses, the insulin/IGF receptor homologue from silkworm (*Bombyx mori*) was used as an outside group.

Results

The IRR gene is expressed in the rat ovary only at the time of the preovulatory surge of gonadotropins

RPA of total RNA from different tissues protected a 428-nt fragment in several tissues. As previously shown (21), there was substantial expression of IRR in the kidney, whole stomach, and the fundus of the stomach (Fig. 1A). No IRR mRNA was detected in the cerebral cortex and liver. Ovaries collected from immature, juvenile rats were also devoid of IRR mRNA. In marked contrast, ovaries collected in the afternoon of the first proestrus had readily detectable IRR mRNA levels (Fig. 1A). By examining ovaries at each stage of the first estrous cycle we determined that IRR mRNA was only expressed in the afternoon of proestrus (Fig. 1B), *i.e.* at the time of the first preovulatory surge of gonadotropins. The mRNA was undetectable after ovulation, *i.e.* on the day of first estrus and continued to be undetectable at the first diestrus (Fig. 1B).

Gonadotropins induce IRR mRNA expression in juvenile ovaries

Juvenile rats treated with PMSG exhibit all the physiologic events that result in ovulation (29, 51). Because the endogenous surge of gonadotropins and ovulation occur at a predictable time, we treated juvenile 26- to 27-d-old rats with a single dose of PMSG to determine whether the increase in IRR mRNA content detected in the ovary in the afternoon of the day of first proestrus was caused by gonadotropins. The preovulatory LH surge is already initiated by 1400 h and reaches peak values by 1800 h of the second day after administration of the PMSG; as in normally cyclic rats, ovulation occurs in the early hours of the day of estrus (51), *i.e.* 8–10 h after the LH surge. Consistent with this afternoon pattern of serum LH levels, the ovarian levels of IRR mRNA measured by RPA were elevated at 1500 h, 54 h after the injection of PMSG, and remained elevated until 2300 h (Fig. 2). To confirm that the elevation of IRR mRNA is accompanied by a subsequent increase in IRR protein, we collected ovaries at

Downloaded from https://academic.oup.com/endo/article/147/1/155/2500201 by Universidad de Chile user on 05 August 2022

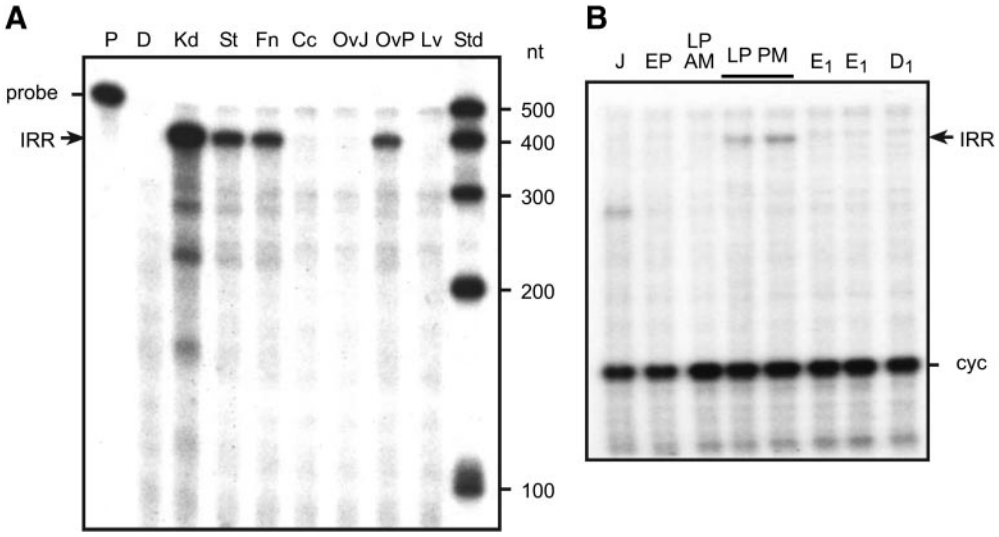

FIG. 1. A, IRR mRNA detected in different tissues by RPA. The 516-nt probe consists of 428 nt transcribed from an IRR cDNA template plus 88 nt derived from transcribed vector sequences. P, Undigested probe; D, digested probe; Kd, kidney; St, stomach; Fn, stomach fundus; Cc, cerebral cortex; OvJ, ovary (juvenile); OvP, ovary (first proestrus); Lv, liver; Std, ^{32}P-labeled RNA ladder. B, IRR mRNA expression in the ovary is restricted to the afternoon of proestrus. The ^{32}P-labeled cRNA probes for IRR and cyclophilin (cyc) (158 nt protected) were hybridized simultaneously to 10 μg total RNA. The ovaries were collected at different stages of the first estrous cycle. J, Juvenile 28-d-old rat; EP, early proestrus (uterine fluid detected); LP AM, late (first) proestrus morning (ballooned uterus weighing more than 200 mg); LP PM, late (first) proestrus (1700 h); E1, first estrus; D1, first diestrus.

2100 h, 2 d after PMSG treatment, and processed one ovary from each animal for measurement of IRR mRNA content and the other for Western blot analysis. As before, the content of IRR mRNA was markedly increased in the ovaries of PMSG-treated rats as compared with saline-injected controls (Fig. 3A). An increase in IRR protein was also apparent (Fig. 3B). The protein species detected was similar in size (68 kDa) as that detected in the kidney, a tissue rich in IRR (23).

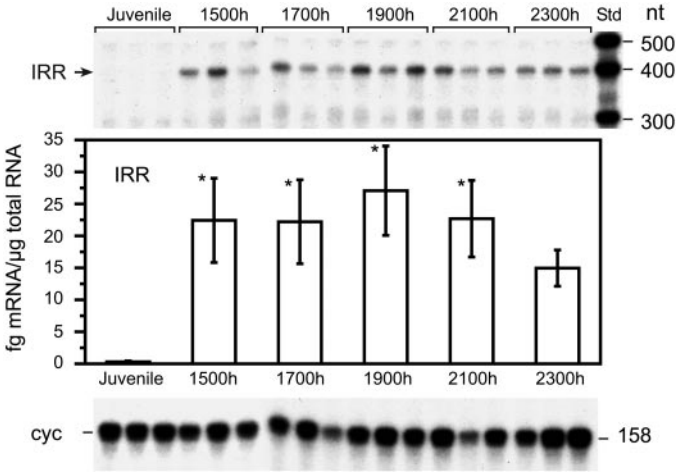

FIG. 2. Ovarian IRR mRNA content measured by RPA increases at the time of the LH surge. Juvenile 26- to 27-d-old rats were injected with PMSG (8 IU, sc), and their ovaries were collected starting 54 h (1500 h) after the injection and every 2 h thereafter, until 2300 h. The LH surge in similarly treated animals occurs at 1700 h (29). IRR mRNA was detected in samples containing 10 μg of total RNA. cyc, Cyclophilin; Std, ^{32}P-labeled RNA ladder. *, $P < 0.05$ *vs.* juvenile.

The prepubertal rat ovary predominantly expresses the mRNA species encoding the full-length IRR

A ^{32}P-labeled RPA probe extending from exon 3 to exon 6 (Fig. 4A) detected all three IRR mRNA isoforms in the PMSG-treated rat ovary. The protected fragments had a size con-

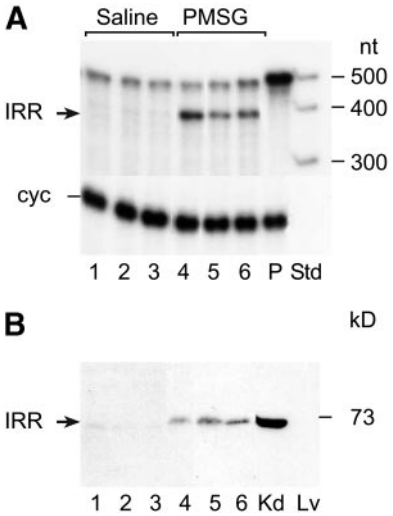

FIG. 3. Ovaries collected from PMSG-treated rats contain more IRR mRNA and IRR protein than those from saline-treated rats. A, IRR mRNA content determined by RPA in one ovary from each animal was increased in PMSG-injected rats compared with saline-injected rats. B, Western blot showing that the ovarian content of an approximate 68-kDa IRR immunoreactive protein species, identical in size to kidney IRR, is increased in the ovaries of PMSG-treated rats (lanes 4–6) compared with saline-injected controls (lanes 1–3). The ovaries were collected 60 h (2100 h) after PMSG or saline injection. cyc, Cyclophilin; Kd, kidney; Lv, liver; P, undigested probe; Std, ^{32}P-labeled RNA ladder.

Downloaded from https://academic.oup.com/endo/article/147/1/155/2500201 by Universidad de Chile user on 05 August 2022

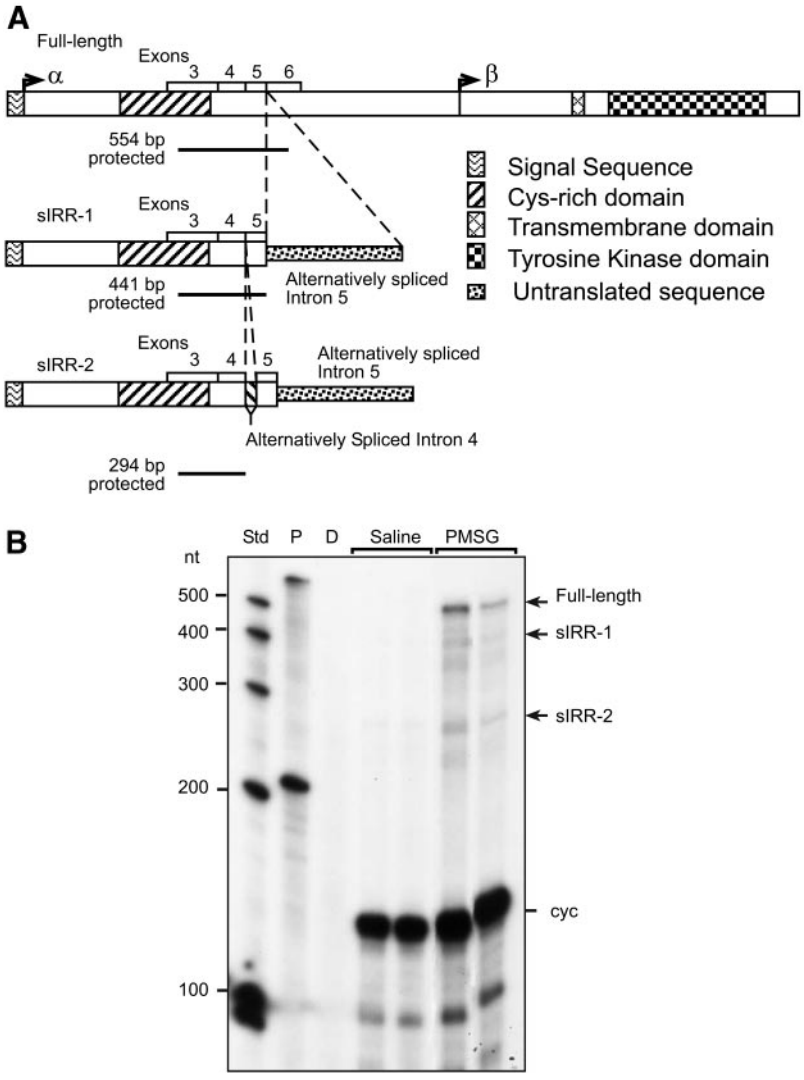

FIG. 4. Splice-variant analysis of ovarian IRR mRNA by RPA. A, Representation of rat IRR, sIRR-1, and sIRR-2 (data derived from Ref. 9). A PCR product spanning exons 3–6 was used as a RPA probe to detect the mRNA encoding the full-length receptor and both splice variants. B, The dominant form of IRR mRNA in the ovary after PMSG treatment (ovaries collected 60 h after injection) is the full-length isoform. The slight signal detected in ovarian RNA from saline-treated rats corresponds to the sIRR-2 splice variant. D, Digested probe; P, undigested probe; Std, ^{32}P-labeled RNA ladder.

sistent with the presence of mRNA species encoding the full-length IRR, as well as the splice variants sIRR-1 and sIRR-2 (Fig. 4B). Despite this, the variant most abundantly expressed after PMSG stimulation was that corresponding to the full-length IRR mRNA (Fig. 4B). The sIRR-2 variant was expressed at much lower levels, and sIRR-1 was present at even lower, almost negligible levels.

The IRR gene is preferentially expressed in thecal-interstitial cells of the preovulatory ovary

To identify the compartment of the ovary where IRR mRNA is expressed, we collected ovaries at 2100 h on the second day after PMSG administration and separated granulosa cells from the rest of the ovarian tissue (residual ovary). Substantially more IRR mRNA was found in the residual ovary compartment containing both thecal and interstitial cells than in granulosa cells (Fig. 5). Hybridization histochemistry confirmed this localization by showing abundant IRR mRNA transcripts in the thecal compartment of antral follicles and interstitial tissue of the ovary (Fig. 6, A and B). Little or no IRR mRNA was detected in granulosa cells, suggesting that the IRR mRNA found in mechanically isolated granulosa cells (Fig. 5) is most likely derived from contaminating thecal-interstitial cells. No hybridization was seen in adjacent sections incubated with a sense IRR probe (Fig. 6, C and D).

Immunohistochemical detection of the IRR protein revealed a distribution identical to that of the mRNA (Fig. 7, A and B), with more abundant levels of the protein present in cells of the theca interna (visualized with more detail in the higher magnification image shown in Fig. 7B). The 727 polyclonal antibodies used for these studies were raised against a synthetic peptide; when antiserum 727 was preadsorbed with its antigenic peptide, all specific immunoreactivity disappeared (Fig. 7C).

PCR and library screening for an insulin-related sequence

Motif-based PCR with degenerate primers and extensive screening of cDNA libraries did not identify an insulin-related sequence different from other members of the insulin family. This method was successfully used to identify a novel cDNA sequence from the gastrointestinal tract of the *P. sauvagei* (47) encoding a peptide sequence with similarity to the insulin family of peptides. Numerous PCRs using cDNAs

Downloaded from https://academic.oup.com/endo/article/147/1/155/2500201 by Universidad de Chile user on 05 August 2022

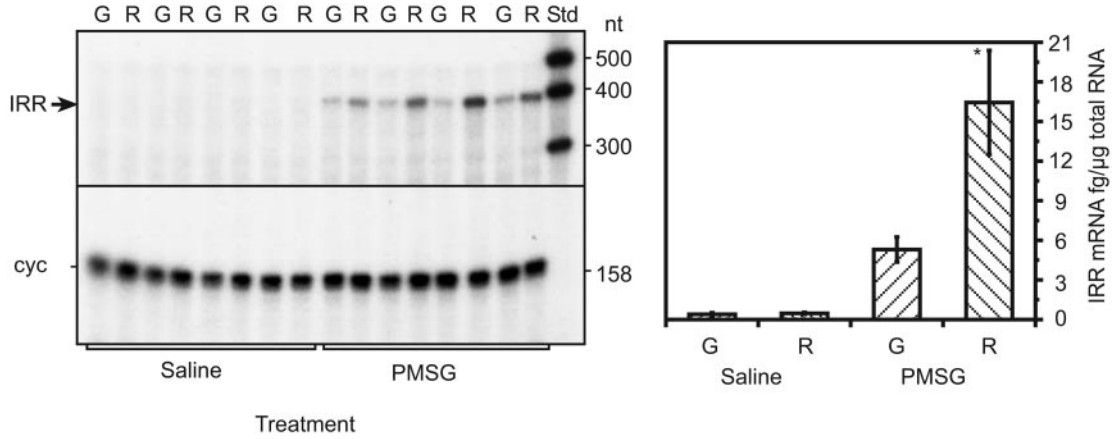

FIG. 5. Most IRR mRNA is detected in the residual ovary and not in granulosa cells. Rats were treated with PMSG (8 IU, sc) and the ovaries removed 60 h later at 2100 h. Follicles were punctured with a 23-gauge needle, and the granulosa cells were expressed by gently pressing the ruptured follicles. The remaining tissue, referred to as the residual ovary, includes mainly thecal and interstitial cells and some contaminating granulosa cells. G, Granulosa cells; R, residual ovary; Std, ^{32}P-labeled RNA ladder. *, $P < 0.05$ *vs.* all other groups.

derived from both reverse-transcribed RNA and cDNA libraries as the template were carried out using various primers and conditions, and yet all failed to isolate a cDNA fragment that was different from the known members of the mammalian insulin family. Hybridization screening of two cDNA libraries also did not yield a novel insulin-related sequence.

A genomic search suggests that the mammalian genome does not contain additional ligands related to the known peptides of the insulin or relaxin families

A genomic search suggests that organisms from insect to human contain multiple insulin/relaxin family peptides. In the *D. melanogaster* genome, there are a total of seven paralogs showing closer sequence similarity to human insulin (52). In contrast, all vertebrates studied contain multiple orthologs for insulin and IGFs as well as human relaxin. In addition to insulin, IGF-I, and IGF-II, the human genome encodes seven peptides belonging to the relaxin subfamily (Fig. 8). Likewise, genomes of teleosts (*Takifugu rubripes* and *Danio rerio*) encoded multiple homologs of insulin, IGFs, and relaxins (Fig. 8). Although the genome search allowed that identification of multiple relaxin subfamily members showing diverged sequences, no sequence exhibiting a close relatedness to known insulin or IGFs was identified in the human genome, suggesting that the human genome encodes only known insulin and *IGF* genes. Based on the notion that ligands and receptors coevolved during evolution, the highly diverged relaxin subfamily peptides are unlikely to function as the IRR ligands. Indeed, recent studies have suggested that all human relaxin subfamily peptides primarily signal through G protein-coupled receptors (53–58), as opposed to the IR and IRR receptors that signal through a tyrosine kinase-dependent mechanism (1).

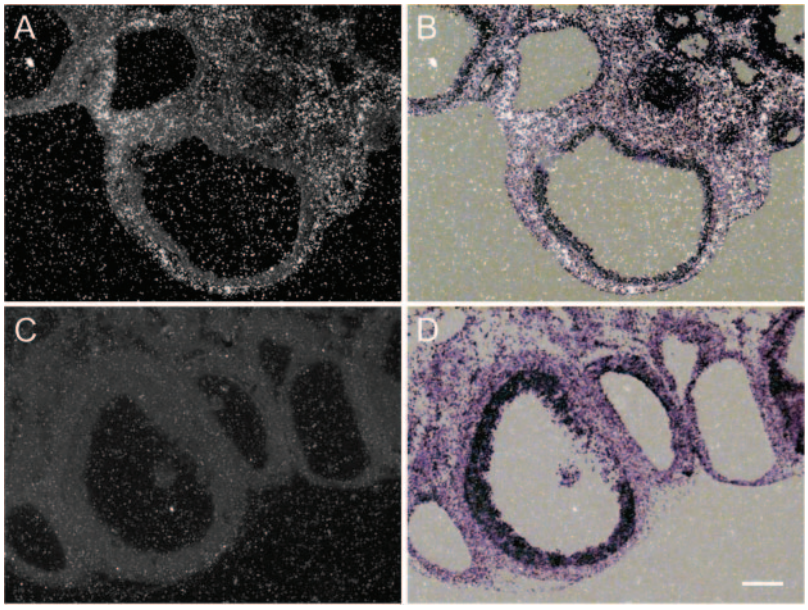

FIG. 6. Cellular localization of IRR mRNA by hybridization histochemistry, using an ^{35}S-labeled IRR cRNA, demonstrates the presence of IRR mRNA transcripts mainly in the thecal layer of large antral follicles and interstitial cells of ovaries from PMSG-treated rats (A and B). A, Illustrates this hybridization pattern in dark-field; B, merged bright- and dark-field images contrasting the abundance of IRR mRNA transcripts in thecal-interstitial cells as compared with granulosa cells. Panels C (dark-field) and D (merged bright- and dark-field images) show the lack of hybridization signals in a section hybridized with an ^{35}S-labeled sense IRR RNA. The ovaries were collected 60 h (2100 h) after PMSG injection. *Bar*, 100 μm.

Downloaded from https://academic.oup.com/endo/article/147/1/155/2500201 by Universidad de Chile user on 05 August 2022

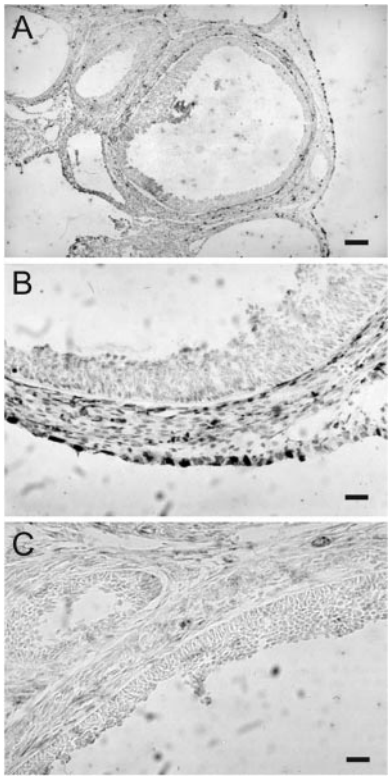

FIG. 7. Immunohistochemical detection of IRR in ovaries of PMSG-treated rats collected 60 h after injection (2100 h). A, Low-magnification image of large preovulatory follicles exhibiting IRR immunoreactive material in thecal cells. B, Higher magnification image of the follicular wall of a preovulatory follicle contrasting the presence of IRR in thecal cells with its absence in granulosa cells. C, Control section incubated with IRR antibodies (antiserum 727) preadsorbed with the IRR antigenic peptide before incubation with the tissue. *Bars*: A and B, 100 μm; C, 25 μm.

In addition to studies of insulin/relaxin family peptides in metazoans, we analyzed the evolution of IRR in vertebrates. Similar to mammals, *X. laevis* contains an IRR ortholog (GenBank accession no. AAH60457) in addition to insulin and IGF-I receptors (IGF-IRs). Phylogenetic analysis based on the full-length or the ectodomain sequences of IR family proteins from human, mouse, *X. laevis*, and silk moth (*B. mori*) indicated that IRR has a closer relatedness to the IGF-IR as compared with the IR (Fig. 9).

Discussion

The ovarian pattern of IRR expression documented in the present study, and that of trkA we reported earlier (29), indicate that expression of both receptors in the ovary is not only regulated in a cell-specific manner, but it is also temporarily coordinated. Our results also demonstrate that the preovulatory surge of gonadotropins is the common factor responsible for the coregulation of both genes. The earlier identification of LH as the gonadotropin that induces ovarian *trkA* gene expression (29), and the present finding of changes in IRR mRNA and protein content restricted to the time of the PMSG-induced surge of endogenous LH, indicates that LH is the gonadotropin triggering both increases. An increase in IRR mRNA abundance also occurs in the afternoon of the first, natural preovulatory surge of gonadotropins. Thus, our findings identify for the first time a physiological mechanism able to simultaneously up-regulate trkA and IRR expression in an endocrine or nervous tissue.

Using both *in situ* hybridization and immunohistochemistry, the IRR was localized to the thecal compartment—the same site of production for trkA receptors in the rat ovary (29). The presence of both receptors on NGF-sensitive thecal cells of the follicular wall, and their increased prevalence during the time of the preovulatory surge of gonadotropins, suggests that the actions of the NGF receptor (trkA) and the IRR on the preovulatory follicle might be functionally cooperative. Genes that participate in a functional pathway or are components of a protein complex are often coregulated exhibiting both coordinated up- and down-regulation (59). The underlying implication of this coordinated control is that the genes involved are functionally cooperative. It has been speculated that coregulatory events observed over large evolutionary distances, and the resulting functional cooperation, create a selective advantage (59). On the other hand, *cis*-regulatory DNA motifs present in genomic regions adjacent to neighboring genes might lead to serendipitous transcriptional coregulation of these genes (59). Although it has yet to be determined which category the *IRR* and *trkA* genes can be grouped into, the present results argue in favor of a specific, hormone-dependent coregulation with functional consequences. The selective advantage of such a tissue- and cell-specific coregulation is obvious because both gene products would cooperate in activating signaling pathways required for ovulation. Although trkA-dependent signaling appears to facilitate follicular rupture (60), the phase(s) of the ovulatory process requiring IRR participation is not known. The possibility that IRR enhances trkA-mediated events leading to ovulatory rupture deserves consideration. Such a cooperative engagement is strongly suggested by the finding that stimulation of trkA receptors results in activation of insulin-dependent signaling pathways, including the phosphorylation of the IR substrates 1 and 2 (IRS-1 and IRS-2), and the association of these substrates with several downstream proteins (such as phosphatidylinositol 3-kinase, growth factor receptor-bound protein 2, and Src homology protein 2), characteristically recruited by insulin/IGF-I binding to their respective receptors (61). It is also possible that IRR activation serves, at least in part, to potentiate IGF-IR-dependent signaling pathways required for ovulation (62).

Because the ligand for IRR has not been identified, defining the functions of the receptor has been more difficult. Our current understanding of the intracellular pathways set in motion by ligand-induced activation of the IRR derives from chimeric receptors wherein the extracellular domain of IRR has been replaced with the extracellular domain of a receptor with a known ligand. The extracellular domains for three different ligands have been used for such studies, namely, insulin (3, 19), colony-stimulating factor-1 (63), and brain derived neurotrophic factor (10, 64). These studies show that IRR activates similar signaling pathways as IR, including stimulation of mitogen-activated protein kinase activity (10), Ser/Thr kinase Akt/PKB (63), phosphatidylinositol 3-kinase (19), and both IRS-1 and IRS-2 (3). The physiological consequences of IRR activation include stimulation of glucose

Downloaded from https://academic.oup.com/endo/article/147/1/155/2500201 by Universidad de Chile user on 05 August 2022

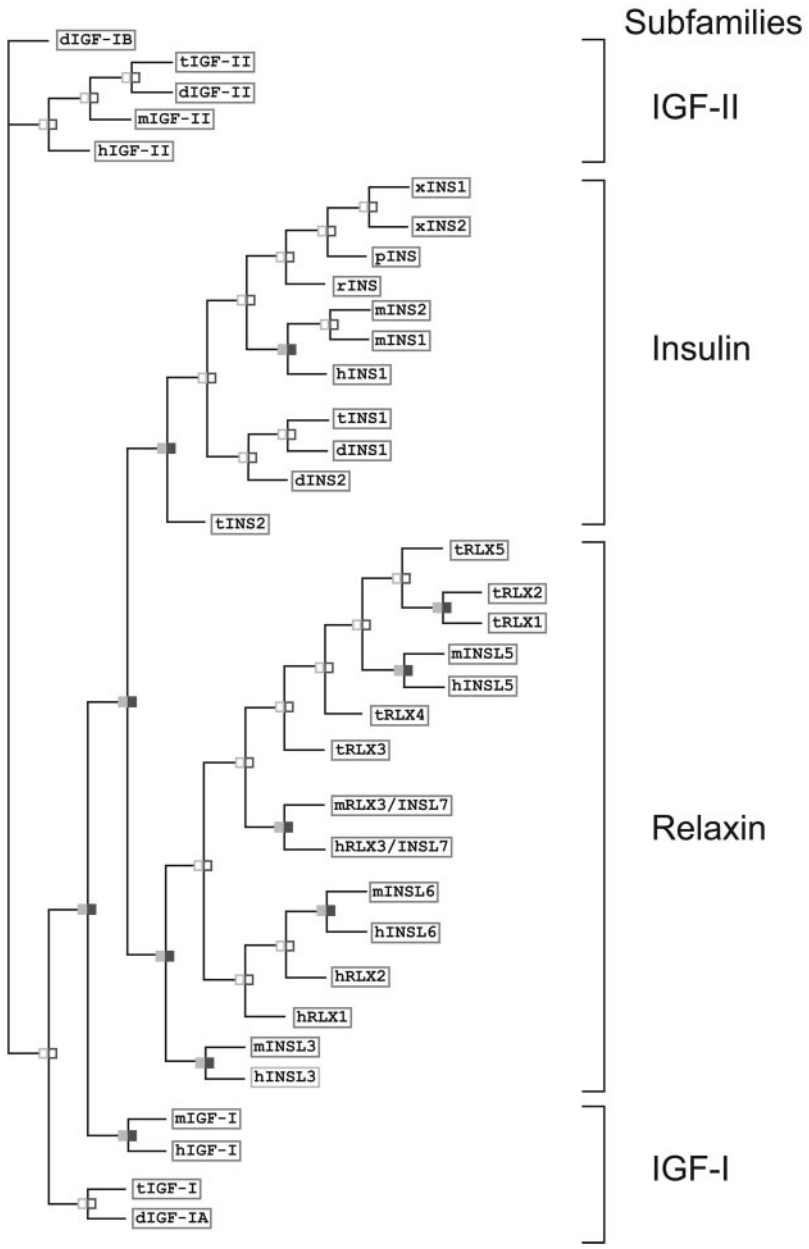

FIG. 8. Phylogenetic analysis of vertebrate insulin/relaxin family peptides. The phylogenetic relationship of vertebrate insulin/relaxin family peptides was studied based on the analysis of mature B and A domain sequences from human, mouse, frog (*P. sauvagei, R. pipiens*, and *X. laevis*), pufferfish (*T. rubripes*), and zebrafish (*D. rerio*). Whereas these species contain a similar number of insulin and *IGF* genes, the inventory of relaxin subfamily paralogs differ greatly among species. For example, the mouse genome contains only five relaxin family genes compared with seven found in humans (72). The pufferfish, *T. rubripes*, also encodes at least five relaxin family genes (fRLX1–5) in addition to two insulin and two *IGF* genes. However, the five pufferfish relaxin family genes are highly conserved and are sequence orthologs of the human and mouse relaxin3/*INSL7* gene (72). Because orthologs for the less-related human relaxin subfamily peptides can be identified in lower vertebrates through sequence analysis, all insulin and IGFs subfamily peptides in the available genomes are likely to be identifiable. Thus, the presence of additional human insulin-like paralogs is unlikely. The GenBank accession numbers for nonmammalian insulin/relaxin family gene orthologs are tIGF-I,CAAB01000259; tIGF-II, CAAB01000017; dIGF-IA, BX510924.10; dIGF-IB, BX548049.9; dIGF-II, AL928880.5; tINS1, CAAB01001780; tINS2, CAAB01002502; dINS1, BX465852.6; dINS2, BX088535.6; tRLX1, CAAB01000252; tRLX2, CAAB01001006; tRLX3, CAAB01001937; tRLX4, CAAB01001213; tRLX5, CAAB01004902; xINS1, AAA49888; xINS2, AAA49887; and rINS, AF227187. d, Zebrafish (*D. rerio*); h, human; m, mouse; p, frog (*P. sauvagei*); r, frog (*R. pipiens*); t, pufferfish (*T. rubripes*); x, frog (*X. laevis*). The human *INSL4* gene (a member of the relaxin subfamily) appeared to be primate specific and was not included in the present analysis.

uptake, inhibition of lipolysis, activation of glycogen synthase, increased thymidine incorporation, enhanced neuronal survival, and differentiation of a neural progenitor cell (10, 19, 63, 64). The importance of the IR-signaling pathways to reproduction is shown by the disruption of the signaling-pathway molecules IRS-1 and IRS-2 by gene targeting. Such a mutation results in a mild reduction of female fertility in the case of IRS-1, and almost complete female infertility in IRS-2 null mutant mice (65).

Although these findings make evident that activation of specific IR-dependent pathways are critical for normal reproductive function, the contribution made by the IRR to the functional integrity of these pathways remains unclear. Disruption of the *IRR* gene does not result in any discernible phenotype. Bodily growth and morphological, reproductive, and gross behavioral parameters are essentially similar in IRR-null mutant and wild-type mice (66); likewise, blood glucose and insulin levels, measured in both fasting and fed states, are normal in IRR-deficient mice (66). In contrast to this lack of associated phenotype, deletion of the IR or IGF-IR led to a very different outcome, because both are necessary for postnatal life; null mutants for these receptors die at birth or within 4 d of birth (reviewed in Ref. 30). Because the IRR has been shown to form hybrid receptors with both IR and IGF-IR, it has been suggested that instead of functioning as an independent receptor, the IRR forms a complex with the other two receptors to initiate intracellular signaling (1, 6, 19, 67, 68). The importance of these interactions was made apparent by the examination of single-, double-, or triple-null mutant embryonic d 18.5 mice lacking IRR, IR, and IGF-IR (30). Whereas the absence of all three receptors resulted in a male to female sex-reversal phenotype, loss of IR and IGF-IR

Downloaded from https://academic.oup.com/endo/article/147/1/155/2500201 by Universidad de Chile user on 05 August 2022

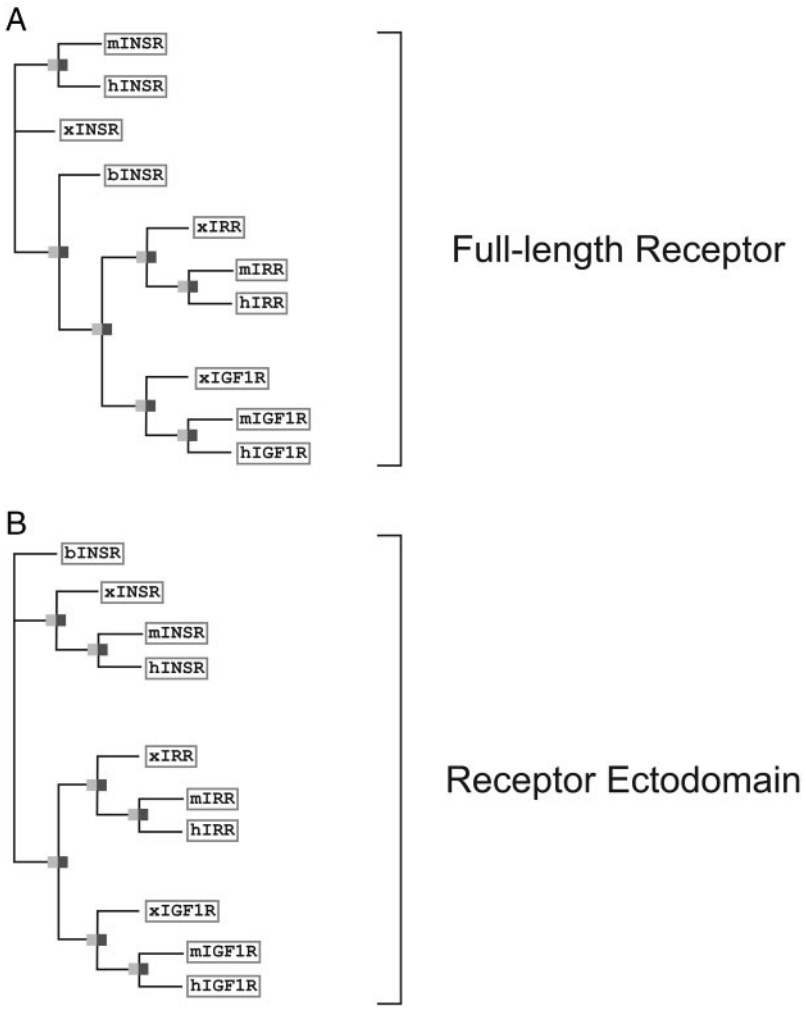

FIG. 9. Phylogenetic analysis of IR family proteins from select model organisms. The phylogenetic relationship of vertebrate IR family proteins was studied based on the analysis of the full-length (A) or the ectodomain (B) sequences of receptors from human, mouse, frog (*X. laevis*), and silk moth (*B. mori*). b, Silk moth (*B. mori*); h, human; m, mouse; x, frog (*X. laevis*). The GenBank accession numbers for nonmammalian receptor sequences are xINSR, CAB46565; xIGF-IR, AAC12942; xIRR, AAH60457; and bINSR, AAF21243.

in the presence of wild-type IRR alleles resulted in only a partially sex-reversed phenotype (30). Therefore, the presence of IRR alone can partially compensate for IR and IGF-IR in male sex determination, a conclusion consistent with the idea that the IRR is part of a redundant signaling pathway initiated by activation of the IR and IGF-IR (19, 30).

Whereas it is clear that IRR can act through the formation of heterodimeric complexes with IR and IGF-IR, IRR appears also capable of independent receptor signaling. In the presence of a monoclonal antibody that forces the formation of homodimer-receptor complexes, it was found that the activated IRR was able to elicit intracellular signaling in the absence of IR and IGF-IR (68). Whether IRR forms heteromeric complexes with trkA receptors is currently unknown.

Our molecular and bioinformatics search for IRR ligands in the mammalian genome did not yield an insulin- or relaxin-related molecule with the potential of being the long-sought-after IRR ligand. These efforts were prompted by other studies in which a combination of motif-based PCR with degenerate primers, and a cDNA library prepared from the gastrointestinal tract of the frog *P. sauvagei*, was used to isolate cDNAs encoding an insulin-like peptide able to stimulate IRR autophosphorylation (47). This peptide lacks the carboxy-terminal extensions characteristic of IGFs, exhibiting instead a short C-peptide domain flanked by dibasic sequences. Using synthetic peptides encoding the predicted A and B chains of this insulin-related protein and rabbit reticulocyte lysates for *in vitro* expression of the protein, it was found that the resulting processed product stimulated autophosphorylation of IR, IGF-IR, and IRR in transfected cell lines (47). Pairwise comparisons showed that the *P. sauvagei* sequence is ortholog to two *X. laevis* insulin sequences (69). Because the two *X. laevis* sequences share 94% similarity among themselves, but only 87% similarity with the *P. sauvagei* sequence (when comparing mature peptide sequences only), it is likely that the *X. laevis* sequences evolved after their evolutionary separation from *P. sauvagei*. In fact, the results of our phylogenetic analysis, including 20 insulin-related sequences and 15 relaxin family peptides from selected vertebrates, demonstrated that the *P. sauvagei* sequence clusters with insulins from *Rana pipiens* and *X. laevis* frogs. Thus, it must have evolved after the divergence of major vertebrate branches, making it unlikely that any other ortholog of the insulin gene exists in the mammalian genome. This conclusion is in contrast to the notion, suggested by the present bioinformatics analysis, that the IRR itself may have evolved from a common ancestor of IGF-R and IRR after this common ancestor separated from IR. Based on the under-

Downloaded from https://academic.oup.com/endo/article/147/1/155/2500201 by Universidad de Chile user on 05 August 2022

standing that ligands coevolve with their cognate receptors and that IRR has a closer relatedness to IGF-R than to IR receptors, one must consider the possibility that diverse IGF isoforms generated through alternative posttranslational cleavage of conserved basic residues (70, 71) may function as IRR ligands.

Additional studies are underway to determine whether trkA and IRR interact physically and/or functionally in the ovary to affect the ovulatory process. As mentioned earlier, the finding that activation of trkA in nonneural cells results in phosphorylation of IRS-1 and IRS-2, the major substrates for insulin and IGF-IRs, and sets in motion several insulin/IGF-I downstream events (61) raises the possibility that both receptors may act cooperatively in the ovary to control ovulatory events.

Acknowledgments

We thank Maria E. Costa for valuable technical expertise in performing the immunohistochemistry and hybridization histochemistry procedures reported here. We also thank Janie Gliessman for editorial assistance.

Received April 4, 2005. Accepted September 17, 2005.

Address all correspondence and requests for reprints to: Gregory A. Dissen, Division of Neuroscience, Oregon Regional Primate Research Center, 505 N.W. 185th Avenue, Beaverton, Oregon 97006-3448. E-mail: disseng@ohsu.edu; or Sergio R. Ojeda, Division of Neuroscience, Oregon Regional Primate Research Center, 505 Northwest 185th Avenue, Beaverton, Oregon 97006-3448. E-mail: ojedas@ohsu.edu.

This work was supported by National Institutes of Health Grant HD24870 (to S.R.O.), the National Institute of Child Health and Human Development through cooperative agreement no. U54 HD18185 as part of the Specialized Cooperative Centers Program in Reproduction Research (to S.R.O.), and National Institutes of Health Grants RR00163, for the operation of the Oregon National Primate Research Center, and HD047606 and HD31398 Core C (to S.-Y.T.H.). C.G.-R. was a visiting scientist supported by a fellowship from the National Institute of Child Health and Human Development, Fogarty International Training & Research in Population & Health grant (TW/HD00668).

Present address for V.T.: Laboratorio de Bioquimica, Departmento de Ob/Gyn, Hospital Clinico, Universidad de Chile, Santos Dumont 999, Santiago, Chile.

References

1. **Shier P, Watt VM** 1989 Primary structure of a putative receptor for a ligand of the insulin family. J Biol Chem 264:14605–14608
2. **Hänze J, Berthold A, Klammt J, Gallaher B, Siebler T, Kratzsch J, Elmlinger M, Kiess W** 1999 Cloning and sequencing of the complete cDNA encoding the human insulin receptor related receptor. Horm Metab Res 31:77–79
3. **Hirayama I, Tamemoto H, Yokota H, Kubo S-K, Wang J, Kuwano H, Nagamachi Y, Takeuchi T, Izumi T** 1999 Insulin receptor-related receptor is expressed in pancreatic β-cells and stimulates tyrosine phosphorylation of insulin receptor substrate-1 and -2. Diabetes 48:1237–1244
4. **Shier P, Watt VM** 1992 Tissue-specific expression of the rat insulin receptor-related receptor gene. Mol Endocrinol 6:723–729
5. **Kurachi H, Jobo K, Ohta M, Kawasaki T, Itoh N** 1992 A new member of the insulin receptor family, insulin receptor-related receptor, is expressed preferentially in the kidney. Biochem Biophys Res Commun 187:934–939
6. **Jui HY, Suzuki Y, Accili D, Taylor SI** 1994 Expression of a cDNA encoding the human insulin receptor-related receptor. J Biol Chem 269:22446–22452
7. **Zhang B, Roth RA** 1991 Binding properties of chimeric insulin receptors containing the cysteine-rich domain of either the insulin-like growth factor I receptor or the insulin receptor related receptor. Biochemistry 30:5113–5117
8. **Watt VM, Shier P, Chan J, Petrisor BA, Mathi SK** 1993 IRR: a novel member of the insulin receptor family. Adv Exp Med Biol 343:125–132
9. **Itoh N, Jobo K, Tsujimoto K, Ohta M, Kawasaki T** 1993 Two truncated forms of rat insulin receptor-related receptor. J Biol Chem 268:17983–17986
10. **Kelly-Spratt KS, Klesse LJ, Merenmies J, Parada LF** 1999 A trkB/insulin receptor-related receptor chimeric receptor induces PC12 cell differentiation and exhibits prolonged activation of mitogen-activated protein kinase. Cell Growth Differ 10:805–812
11. **Sacristán MP, de Diego JG, Bonilla M, Martin-Zanca D** 1999 Molecular cloning and characterization of the 5′-region of the mouse *trk*A proto-oncogene. Oncogene 18:5836–5842
12. **Ma L, Merenmies J, Parada LF** 2000 Molecular characterization of the TrkA/NGF receptor minimal enhancer reveals regulation by multiple *cis* elements to drive embryonic neuron expression. Development 127:3777–3788
13. **Shier P, Willard HF, Watt VM** 1990 Localization of the insulin receptor-related receptor gene to human chromosome 1. Cytogenet Cell Genet 54:80–81
14. **Valent A, Danglot G, Bernheim A** 1997 Mapping of the tyrosine kinase receptors trkA (NTRK1), trkB (NTRK2) and trkC (NTRK3) to human chromosomes 1q22, 9q22, and 15q25 by fluorescence in situ hybridization. Eur J Hum Genet 5:102–104
15. **Reinhardt RR, Chin E, Zhang B, Roth RA, Bondy CA** 1994 Selective coexpression of insulin receptor-related receptor (IRR) and TRK in NGF-sensitive neurons. J Neurosci 14:4674–4683
16. **Tsuji N, Tsujimoto K, Takada N, Ozaki K, Ohta M, Itoh N** 1996 Expression of insulin receptor-related receptor in the rat brain examined by in situ hybridization and immunohistochemistry. Brain Res Mol Brain Res 41:250–258
17. **Tsujimoto K, Tsuji N, Ozaki K, Minami M, Satoh M, Itoh N** 1995 Expression of insulin receptor-related receptor mRNA in the rat brain is highly restricted to forebrain cholinergic neurons. Neurosci Lett 188:105–108
18. **Kordower JH, Chen E-Y, Sladek Jr JR, Mufson EJ** 1994 Trk-immunoreactivity in the monkey central nervous system: forebrain. J Comp Neurol 349:20–35
19. **Zhang B, Roth RA** 1992 The insulin receptor-related receptor. J Biol Chem 267:18320–18328
20. **Reinhardt RR, Chin E, Zhang B, Roth RA, Bondy CA** 1993 Insulin receptor-related receptor messenger ribonucleic acid is focally expressed in sympathetic and sensory neurons and renal distal tubule cells. Endocrinology 133:3–10
21. **Mathi SK, Chan J, Watt VM** 1995 Insulin receptor-related receptor messenger ribonucleic acid: quantitative distribution and localization to subpopulations of epithelial cells in stomach and kidney. Endocrinology 136:4125–4132
22. **Shibayama E, Koizumi H** 1996 Cellular localization of the Trk neurotrophin receptor family in human non-neuronal tissues. Am J Pathol 148:1807–1818
23. **Bates CM, Merenmies JM, Kelly-Spratt KS, Parada LF** 1997 Insulin receptor-related receptor expression in non-A intercalated cells in the kidney. Kidney Int 51:674–681
24. **Ozaki K, Takada N, Tsujimoto K, Tsuji N, Kawamura T, Muso E, Ohta M, Itoh N** 1997 Localization of insulin receptor-related receptor in the rat kidney. Kidney Int 52:694–698
25. **Kanaka-Gantenbein C, Tazi A, Czernichow P, Scharfmann R** 1995 *In vivo* presence of the high affinity nerve growth factor receptor *trk*-A in the rat pancreas: differential localization during pancreatic development. Endocrinology 136:761–769
26. **Ozaki K** 1998 Insulin receptor-related receptor in rat islets of Langerhans. Eur J Endocrinol 139:244–247
27. **Hannestad J, García-Suárez O, Huerta JJ, Naves EFJ, Vega JA** 1997 TrkA neurotrophin receptor protein in the rat and human thymus. Anat Rec 249: 373–379
28. **García-Suárez O, Germanà A, Hannestad J, Ciriaco E, Laurà R, Naves J, Esteban I, Silos-Santiago I, Vega JA** 2000 TrkA is necessary for the normal development of the murine thymus. J Neuroimmunol 108:11–21
29. **Dissen GA, Hill DF, Costa ME, Dees WL, Lara HE, Ojeda SR** 1996 A role for *trk*A nerve growth factor receptors in mammalian ovulation. Endocrinology 137:198–209
30. **Nef S, Verman-Kurvari S, Merenmies J, Vassalli J-D, Efstratiadis A, Accill D, Parada LF** 2003 Testis determination requires insulin receptor family function in mice. Nature 426:291–295
31. **Ojeda SR, Wheaton JE, Jameson HE, McCann SM** 1976 The onset of puberty in the female rat. I. Changes in plasma prolactin, gonadotropins, LHRH levels and hypothalamic LHRH content. Endocrinology 98:630–638
32. **Urbanski HF, Ojeda SR** 1985 The juvenile-peripubertal transition period in the female rat: establishment of a diurnal pattern of pulsatile luteinizing hormone secretion. Endocrinology 117:644–649
33. **Aguado LI, Ojeda SR** 1984 Prepubertal ovarian function is finely regulated by direct adrenergic influences. Role of the adrenergic innervation. Endocrinology 114:1845–1853
34. **Chomczynski P, Sacchi N** 1987 Single-step method of RNA isolation by acid guanidinium thiocyanate-phenol-chloroform extraction. Anal Biochem 162: 156–159
35. **Danielson PE, Forss-Petter S, Brow MA, Calavetta L, Douglass J, Milner RJ, Sutcliffe JG** 1988 p1B15: a cDNA clone of the rat mRNA encoding cyclophilin. DNA 7:261–267
36. **Mayerhofer A, Danilchik M, Pau K-YF, Lara HE, Russell LD, Ojeda SR** 1996 Testis of prepubertal rhesus monkeys receives a dual catecholaminergic input provided by the extrinsic innervation and an intragonadal source of catecholamines. Biol Reprod 55:509–518
37. **Gilman M** 1993 Ribonuclease protection assay. In: Ausubel FM, Brent R, Kingston RE, Moore DD, Seidman JG, Smith JA, Struhl K, eds. Current protocols in molecular biology. Vol 1. New York: Green Publishing Assoc. and Wiley-Interscience; 4.7.1–4.7.6
38. **Hill DF, Dissen GA, Ma YJ, Ojeda SR** 1992 Detection of nerve growth factor

Downloaded from https://academic.oup.com/endo/article/147/1/155/2500201 by Universidad de Chile user on 05 August 2022

and one of its receptors. In: Conn PM, ed. Methods in neurosciences. Vol 9. Gene expression in neural tissues. New York: Academic Press; 179–196
39. **Lara HE, Hill DF, Katz KH, Ojeda SR** 1990 The gene encoding nerve growth factor is expressed in the immature rat ovary: effect of denervation and hormonal treatment. Endocrinology 126:357–363
40. **Ojeda SR, Hill DF, Katz KH** 1991 The genes encoding nerve growth factor and its receptor are expressed in the developing female rat hypothalamus. Mol Brain Res 9:47–55
41. **Milner RJ, Sutcliffe JG** 1983 Gene expression in rat brain. Nucleic Acids Res 11:5497–5520
42. **Dissen GA, Newman Hirshfield A, Malamed S, Ojeda SR** 1995 Expression of neurotrophins and their receptors in the mammalian ovary is developmentally regulated: changes at the time of folliculogenesis. Endocrinology 136: 4681–4692
43. **Correa-Rotter R, Mariash CN, Rosenberg ME** 1992 Loading and transfer control for Northern hybridization. Biotechniques 12:154–158
44. **Prevot V, Cornea A, Mungenast A, Smiley G, Ojeda SR** 2003 Activation of erbB-1 signaling in tanycytes of the median eminence stimulates transforming growth factor β_1 release via prostaglandin E2 production and induces cell plasticity. J Neuroscience 23:10622–10632
45. **Simmons DM, Arriza JL, Swanson LW** 1989 A complete protocol for *in situ* hybridization of messenger RNAs in brain and other tissues with radiolabeled single-stranded RNA probes. J Histotechnol 12:169–181
46. **Dissen GA, Hill DF, Costa ME, Ma YJ, Ojeda SR** 1991 Nerve growth factor receptors in the peripubertal rat ovary. Mol Endocrinol 5:1642–1650
47. **Nagalla SR, Pattee P, Roberts Jr CT**, Cloning and characterization of a novel amphibian insulin-like peptide from *Phyllomedusa sauvagei,* Program of the 79th Annual Meeting of The Endocrine Society, Minneapolis, MN, 1997, p 566 (Abstract 519)
48. **Quertermous T** 1996 Plating libraries and transfer to filter membranes. In: Ausubel FM, Brent R, Kingston RE, Moore DD, Seidman JG, Smith JA, Struhl K, eds. Current protocols in molecular biology. Vol 1. New York: John Wiley & Sons, Inc.; 6.1.1–6.2.3
49. **Strauss WM** 1993 Hybridization with radioactive probes. In: Ausubel FM, Brent R, Kingston RE, Moore DD, Seidman JG, Smith JA, Struhl K, eds. Current protocols in molecular biology. Vol 1. New York: John Wiley & Sons, Inc.; 6.3.1–6.3.6
50. **Tabor S, Struhl K, Scharf SJ, Gelfand DH** 1994 DNA-dependent DNA polymerases. In: Ausubel FM, Brent R, Kingston RE, Moore DD, Seidman JG, Smith JA, Struhl K, eds. Current protocols in molecular biology. Vol 1. New York: John Wiley & Sons, Inc.; 3.5.1.–3.5.15
51. **Parker Jr CR, Costoff A, Muldoon TG, Mahesh VB** 1976 Actions of pregnant mare serum gonadotropin in the immature female rat: correlative changes in blood steroids, gonadotropins, and cytoplasmic estradiol receptors of the anterior pituitary and hypothalamus. Endocrinology 98:129–138
52. **Ikeya T, Galic M, Belawat P, Nairz K, Hafen E** 2002 Nutrient-dependent expression of insulin-like peptides from neuroendocrine cells in the CNS contributes to growth regulation in Drosophila. Curr Biol 12:1293–1300
53. **Hsu SY, Nakabayashi K, Nishi S, Kumagai J, Kudo M, Sherwood OD, Hsueh AJ** 2002 Activation of orphan receptors by the hormone relaxin. Science 295: 671–674
54. **Kumagai J, Hsu SY, Matsumi H, Roh JS, Fu P, Wade JD, Bathgate RA, Hsueh AJ** 2002 INSL3/Leydig insulin-like peptide activates the LGR8 receptor important in testis descent. J Biol Chem 277:31283–31286
55. **Sudo S, Kumagai J, Nishi S, Layfield S, Ferraro T, Bathgate RA, Hsueh AJ** 2003 H3 relaxin is a specific ligand for LGR7 and activates the receptor by interacting with both the ectodomain and the exoloop 2. J Biol Chem 278: 7855–7862
56. **Liu C, Chen J, Sutton S, Roland B, Kuei C, Farmer N, Sillard R, Lovenberg TW** 2003 Identification of relaxin-3/INSL7 as a ligand for GPCR142. J Biol Chem 278:50765–50770
57. **Liu C, Eriste E, Sutton S, Chen J, Roland B, Kuei C, Farmer N, Jornvall H, Sillard R, Lovenberg TW** 2003 Identification of relaxin-3/INSL7 as an endogenous ligand for the orphan G-protein-coupled receptor GPCR135. J Biol Chem 278:50754–50764
58. **Liu C, Kuei C, Sutton S, Chen J, Bonaventure P, Wu J, Nepomuceno D, Kamme F, Tran DT, Zhu J, Wilkinson T, Bathgate R, Eriste E, Sillard R, Lovenberg TW** 2005 INSL5 is a high affinity specific agonist for GPCR142 (GPR100). J Biol Chem 280:292–300
59. **Stuart JM, Segal E, Koller D, Kim SK** 2003 A gene-coexpression network for global discovery of conserved genetic modules. Science 302:249–255
60. **Mayerhofer A, Dissen GA, Parrott JA, Hill DF, Mayerhofer D, Garfield RE, Costa ME, Skinner MK, Ojeda SR** 1996 Involvement of nerve growth factor in the ovulatory cascade: *Trk*A receptor activation inhibits gap-junctional communication between thecal cells. Endocrinology 137:5662–5670
61. **Miranda C, Greco A, Miele C, Pierotti MA, Van Obberghen E** 2001 IRS-1 and IRS-2 are recruited by TrkA receptor and oncogenic TRK-T1. J Cell Physiol 186:35–46
62. **Baker J, Hardy MP, Zhou J, Bondy C, Lupu F, Bellvé AR, Efstratiadis A** 1996 Effects of an *Igf1* gene null mutation on mouse reproduction. Mol Endocrinol 10:903–918
63. **Dandekar AA, Wallach BJ, Barthel A, Roth RA** 1998 Comparison of the signaling abilities of the cytoplasmic domains of the insulin receptor and the insulin receptor-related receptor in 3T3-L1 adipocytes. Endocrinology 139: 3578–3584
64. **Kelly-Spratt KS, Klesse LJ, Parada LF** 2002 BDNF activated TrkB/IRR receptor chimera promotes survival of sympathetic neurons through Ras and PI-3 kinase signaling. J Neurosci Res 69:151–159
65. **Burks DJ, Font deMora J, Schubert M, Withers DJ, Myers MG, Towery HH, Altamuro SL, Flint CL, White MF** 2000 IRS-2 pathways integrate female reproduction and energy homeostasis. Nature 407:377–382
66. **Kitamura T, Kido Y, Nef S, Merenmies J, Parada LF, Accili D** 2001 Preserved pancreatic β-cell development and function in mice lacking the insulin receptor-related receptor. Mol Cell Biol 21:5624–5630
67. **Jui HY, Accili D, Taylor SI** 1996 Characterization of a hybrid receptor formed by dimerization of the insulin receptor-related receptor (IRR) with the insulin receptor (IR): coexpression of cDNAs encoding human IRR and human IR in NIH-3T3 cells. Biochemistry 35:14326–14330
68. **Kovacina KS, Roth RA** 1995 Characterization of the endogenous insulin receptor-related receptor in neuroblastomas. J Biol Chem 270:1881–1887
69. **Shuldiner AR, Phillips S, Roberts Jr CT, LeRoith D, Roth J** 1989 Xenopus laevis contains two nonallelic preproinsulin genes. cDNA cloning and evolutionary perspective. J Biol Chem 264:9428–9432
70. **Duguay SJ, Milewski WM, Young BD, Nakayama K, Steiner DF** 1997 Processing of wild-type and mutant proinsulin-like growth factor-IA by subtilisin-related proprotein convertases. J Biol Chem 272:6663–6670
71. **Duguay SJ, Jin Y, Stein J, Duguay AN, Gardner P, Steiner DF** 1998 Post-translational processing of the insulin-like growth factor-2 precursor. Analysis of O-glycosylation and endoproteolysis. J Biol Chem 273:18443–18451
72. **Hsu SY** 2003 New insights into the evolution of the relaxin-LGR signaling system. Trends Endocrinol Metab 14:303–309

***Endocrinology* is published monthly by The Endocrine Society (http://www.endo-society.org), the foremost professional society serving the endocrine community.**

Downloaded from https://academic.oup.com/endo/article/147/1/155/2500201 by Universidad de Chile user on 05 August 2022